

# DYNAMIC FRICTION EXPERIMENTS AT THE ATLAS PULSED POWER FACILITY\*

C. L. Rousculp, J. E. Hammerberg, D. M. Oro, G. Rodriguez, P. M. Goodwin,  
M. A. Salazar, R. E. Reinovsky, R. J. Faehl, R. Chartrand  
*Los Alamos National Laboratory, Los Alamos, New Mexico, USA*

J. R. Becker, R. A. Berglin, K. W. Delzer, G. H. Gomez, R. M. Malone, D. V. Morgan,  
T. V. Pate, K. E. Theuer  
*NSTec, Nevada, USA*

D. A. Rigney, H. J. Kim  
*The Ohio State University, Columbus, Ohio, USA*

## Abstract

A Series of dynamic friction experiments has been conducted at the Atlas Pulsed Power Facility. Pulsed currents in excess of 21 MAmps were delivered to a cylindrical liner in about 15 ms. The liner was accelerated to km/s velocities and symmetrically impacted a hollow Ta/Al/Ta target. Due to the shock speed difference in Ta and Al, sliding velocities of almost a km/s were achieved at the Ta/Al interfaces. Initial analysis indicates that the machine performed to within a few percent of the design specifications. The primary diagnostic for these experiments was three radiographic lines-of-sight to look at thin gold wires embedded within the Al piece of the target. The magnitude of the displacement and the amount of distortion of the wires near the material interface is used as a measure of the dynamic frictional forces occurring there. Other diagnostics included a single-point VISAR and line-ORVIS to measure the breakout time and velocity on the inside of the target. Also, the Faraday rotation of a laser beam through a circular loop of optical fiber located in the power-flow channel of the experiment is used to measure the total current delivered to the experimental load. Data are being compared to a theoretical dynamic friction model for high sliding velocities. The model is based on molecular dynamics simulations and predicts an inverse power law dependence of frictional forces at very high sliding.

## I. INTRODUCTION

Computational Lagrangian hydrodynamics utilizes the notion that mass neither flows in nor out of a computational cell during the course of a calculation. Thus the mesh is locked to the flow and material boundaries are associated with mesh edges. The shortcoming of this method, when treating multiple

materials under tangential shear at an interface, is that it causes mesh tangling even when it is known that two materials would slide across each other. One method of treating this problem is to represent each material with its own mesh and specify the interaction in terms of normal and tangential forces. This is typically referred to as a slide-line or slip-line treatment[1]. This method is diagramed in Fig. 1. The top and bottom cells represent different materials, which are in physical contact. The slip-line method treats the two materials as separate meshes and calculates nodal interaction forces based on bulk properties. While the normal forces can easily be calculated to satisfy Newton's Laws, the calculation of tangential forces is difficult[2]. This is because the physical phenomena which give rise to tangential forces happen on a scale size much smaller than the dimensions of a computational cell. Frictional forces are dictated by physics on the atomic scale  $10^3$ 's of nm, while computational cell sizes are typically on the order of 0.1 mm.

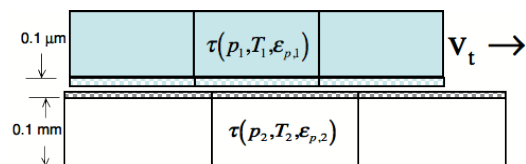


**Figure 1.** Sketch of Lagrangian mesh representation, with slip-line, of the interface between two materials translating at velocity,  $v_t$ , with respect to one-another. The checkered region represents the region over which frictional forces are generated.

The challenge then is to develop a computational model that relates the solid state physics of crystal structure, phonons, and dislocations to the bulk properties of flow stress,  $\tau$ , pressure,  $p$ , temperature,  $T$ , and plastic strain,  $\epsilon_p$ ,

\* This work supported by the U.S. Department of Energy under contract DE-AC52-06NA25396

along with the transverse sliding velocity,  $v$ , and a critical velocity,  $v_c$ . One such model that has been proposed is of the form in Eqn. 1.

$$\frac{F_t}{A} = \tau_w(p, T, \epsilon_p) f(v, v_c) \quad (1)$$

Here,  $F_t$  is the tangential force,  $A$  is the surface area,  $\tau_w$  is the flow stress from the weaker of the two materials. The form of the sliding term,  $f(v, v_c)$  is guided by results from computational molecular dynamics (MD)[3] which is sketched out in Fig 2. There are two regimes dependent on the sliding velocity,  $v$ . At low sliding velocities, there is a positive linear dependence due to phonon dissipation and dislocation dynamics. However, at high sliding velocities, there exists an inverse power-law dependence due to micro-structural transformation of the interface. The exponent of the inverse power-law is predicted to be  $-3/4$  for most ductile metals. It is this velocity weakening which the Atlas Friction 101-103 series of experiments seeks to quantify.

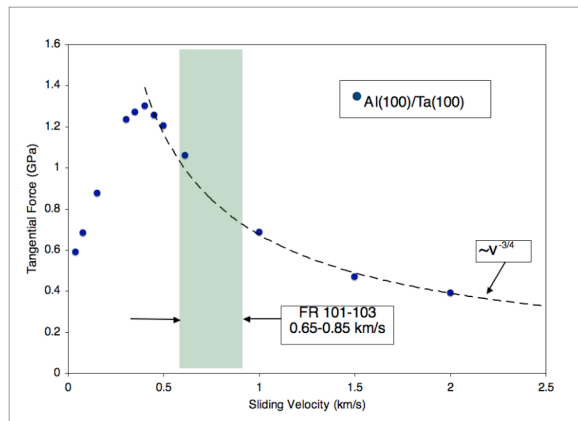


**Figure 2.** Plot of the results from MD simulations of the dependence of tangential frictional forces on sliding velocity. The Atlas FR experiments are designed to explore the high sliding velocity regime and confirm a  $v^{-3/4}$  dependency.

## II. EXPERIMENT DESIGN

The Friction 101-103 series of experiments use a liner-on-target cylindrical configuration with the target composed of a sandwich of tantalum/aluminum/tantalum rings. The design permits two interfaces per experiment and the hollow core allows access for a single-point VISAR and line-ORVIS[4] diagnostics via a central measuring unit (CMU) with turning mirrors. The goal of each experiment is to simultaneously shock the outside of each layer of the target with the aluminum liner. The differential shock speed in aluminum and tantalum creates a strong shear at the interface. By conducting a series of three experiments at different shear velocities the confirmation of the theoretical model can be achieved. The liner has an 80 mm inside diameter and is 7 mm thick

initially. At impact it should be 10 mm thick in order to maintain the shocked state in the two materials for as long as possible. The target is 50 mm in diameter with a 20 mm hole for the CMU. Two sets of four 400 micron diameter gold wires are imbedded in the Al disk at each of three  $120^\circ$  azimuthal offsets so each is viewable by one of three independently timed radial-radiographic lines of sight. Shown in Fig. 3 is a static radiograph of the experimental package along one of the lines of sight.

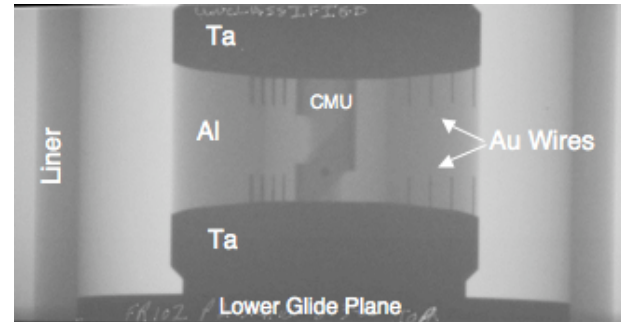


**Figure 3.** Static transverse radiograph showing the liner, lower glide-plane, lifesaver sandwich target of Ta/Al/Ta, embedded Au wires, and CMU.

The balance of this paper is dedicated to the preliminary analysis of the experimental data from the three FR experiments, which were performed at the Atlas Pulsed Power Facility at the Nevada Test Site (APPF-NTS) between April and June of 2006. Comparisons are made to design calculations performed with the 1D Lagrangian MHD code, RAVEN[5]

## III. FARADAY ROTATION

The Faraday rotation diagnostic measures the total current to the experimental load. It is directly comparable to design calculations and thus is a good measure of the quality of the experiment. It consists of two circular loops of fiber optic cable located in a notch in the power-flow channel. The two cables are independent for redundancy and are parallel to the magnetic field. The plane of polarization of a laser beam inside the fiber is rotated depending on the strength of the magnetic field. Fig. 4 shows a plot of the analyzed Faraday data from FR 102 where the peak current was 19 MAmps. The expected current from the design calculation is shown for comparison. The two plots agree within 2% for the duration of the experiment. Data from FR 101 and 103 show similar good agreement.

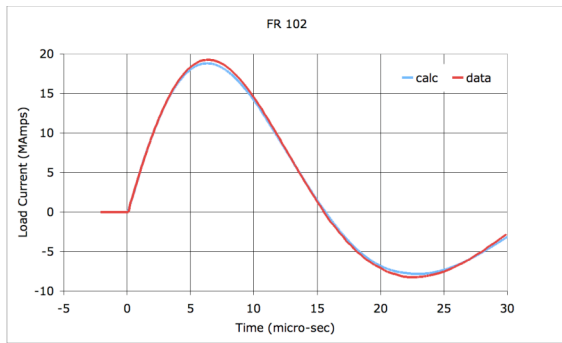


**Figure 4.** Plot of total load current obtained from the Faraday rotation diagnostic and from design calculation for FR 102. Data from FR 101 and 103 show similar good agreement with design calculations.

#### IV. RADIOGRAPHY

Radial radiography provides a time sequence of the bending of embedded Au wires via three independently timed lines of sight ( $\delta t_{pulse} \sim 20$  ns). Shown in Fig 5. is one radiograph ( $t = 22.21 \mu\text{s}$  from current start) along with a close-up of the upper set of Au wires. Comparing with Fig. 3 shows the liner has impacted the target and the shock has just traversed the Al disk. The close-up shows the translation and bending of the Au wires due to frictional forces at the Ta/Al interface.

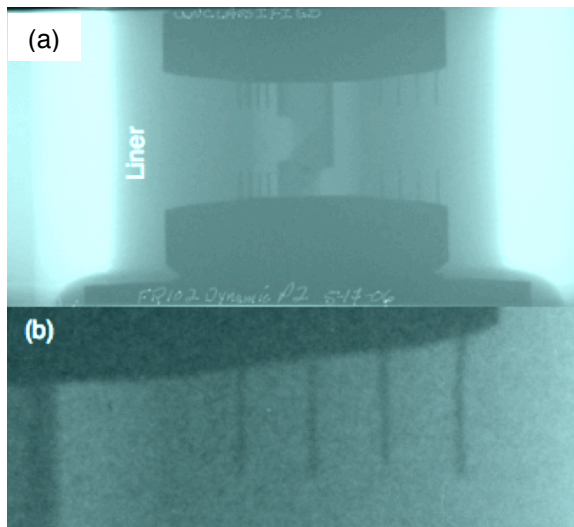


**Figure 5.** Radial Radiography from FR 102. (a) One of three dynamic radiographs taken at  $t = 22.21$  ms after current start. (b) Close-up of the upper-right set of Au wires from (a) showing distinct bending near the interface.

Currently, an advanced noise-reduction, image-analysis technique is being applied to the data. While total variation denoising preserves edges, it can cause long thin features to be lost. By minimizing the “1/2-variation”

edge length is preserved[6]. The ultimate goal is to reduce the uncertainty in the location and shape of the gold wires.

#### V. POINT VISAR

The single-point VISAR diagnostic measures the shock breakout at the inner surface of the target. It is positioned to look at the mid-plane of the Al disk so as to reduce the effects of friction at the Ta/Al interfaces. Fig. 6 shows a comparison plot of the VISAR data and the design calculation. Good agreement is seen between the calculated and measured breakout velocity ( $\sim 1.7$  km/s), however, there is a noticeable difference ( $\sim 200$  ns) between the calculated and measured breakout time ( $21.5 \mu\text{s}$  vs.  $21.8 \mu\text{s}$ ). This result is confirmed by measuring the inner-surface diameter in the radial radiography. The same breakout timing difference is found in the FR 101 and 103 data.

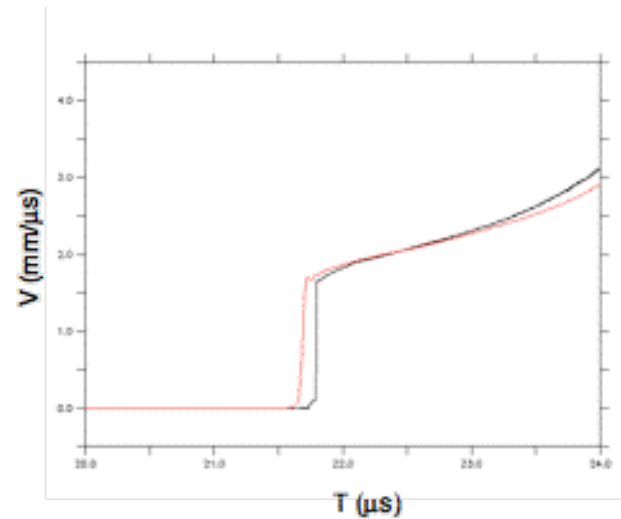


**Figure 6.** Plot of single-point VISAR data from FR 102 (black) and design calculation (red). There is approximately a 200 ns difference in the inner-surface breakout time. Timing is referenced to current start. Data from FR 101 and 103 showed similar behavior.

#### VI. RECOVERED TARGETS

Surprisingly, all three targets were recovered from the experiments. This allows for the post-shot metallurgical analysis of the Ta/Al interface. The targets were first radiographed then sectioned. Fig. 7. Shows the recovered target, radiograph and section. Currently, scanning electron microscopy is being performed to look at the interface with the hope of structural comparison to MD simulations.

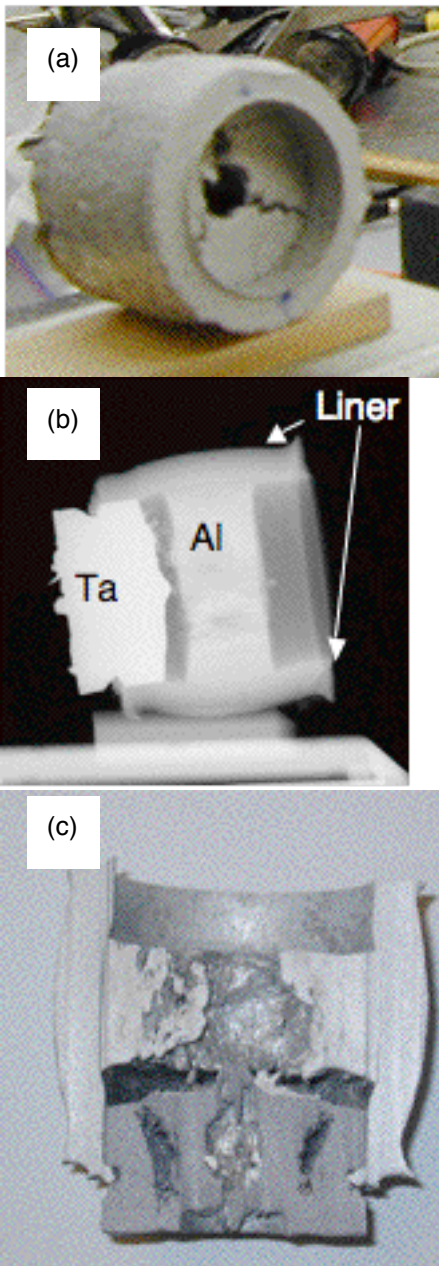


**Figure 7.** (a) Photograph of the FR 103 recovered target. (b) Radiograph revealing the major components. (c) Photograph of the sectioned target showing the inner structure.

## VII. FRICTIONAL FORCE ANALYSIS

A series of 2D Lagrangian hydrodynamic calculations have been performed utilizing the inferred impact velocities from the three experiments. A parameterized constant frictional force is applied at the interface and a best match of the Lagrangian mesh lines to the measured shape and translation of the gold wires is made. Fig. 8 shows a typical calculation.

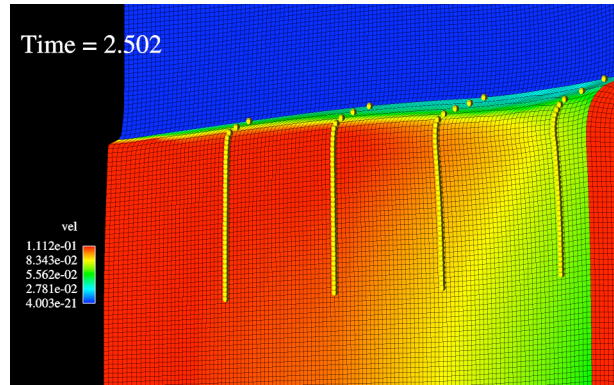


**Figure 8.** A typical 2D Lagrangian hydrodynamics calculation of the FR series experiments. The location of the gold wires is marked by yellow balls. The Ta is in blue, while the Al is colored by velocity.

The second wire from the right as seen in Fig. 8 is used in the analysis. Tab. 1 summarizes the results of the frictional analysis. The key result is that frictional force,  $F_{\text{tang}}/A$ , is decreasing as the interface velocity,  $\langle v_{\text{int}} \rangle$ , is increasing.

Experiment	FR 102	FR 103	FR 101
$V_{\text{impact}}$ (mm/ $\mu$ s)	1.3	1.5	1.7
P (GPa)	13	15	18
Dt	3.58	3.727	2.408
$F_{\text{tang}}/A$ (GPa)	0.60	0.09	< 0.09
Y (GPa)	0.8	0.9	1.0
$\langle v_{\text{int}} \rangle$ (mm/ $\mu$ s)	0.36	0.56	0.70

**Table 1.** Results of preliminary analysis of frictional forces for FR 101-103

## VIII. CONCLUSIONS

Atlas FR 101-103 were successfully conducted at the Atlas Pulsed-Power Facility at the Nevada Test Site between April and June of 2006. The critical diagnostics all performed nominally and show data in good agreement with design specifications. The Faraday rotation diagnostic measured the total-load current to be within 2% of the design calculation for all three shots. The single-point VISAR measured the shock breakout velocity and time from the inner-surface of the target at the mid-plane. The velocity is in good agreement with the design calculations, while the timing shows a systematic 100-200 ns delay. The radial radiography gave a high-contrast sequence of images for each shot. The images show the distinct translation and bending of the Au wires due to frictional forces. Advanced de-noising algorithms are being applied to reduce uncertainty.

Preliminary analysis, based on comparison to computational modeling has confirmed the velocity weakening effect at high sliding velocities.

## IX. REFERENCES

- 
- [1] Wilkins, M. L., *Computer Simulation of Dynamic Phenomena*, Springer, 1999, Chpt. 5.
  - [2] Barlow, A. J., "Friction in CORVUS a 2D ALE Code," *22<sup>nd</sup> International Symposium on Shock Waves*, 1999, paper 2450.
  - [3] Hammerberg, J. E., and Holian, B. L., in *Surface Modification and Mechanisms*, Ed. Toffen and Liang, 2004, pp. 723.
  - [4] Malone, R. M. et al., "ATLAS Line-Imaging ORVIS Diagnostic," *Proceedings of the 15<sup>th</sup> IEEE International Pulsed Power Conference*, Monterrey, 2005.
  - [5] Oliphant, T. A. and Witte, K. H., *RAVEN*, Los Alamos National Laboratory Publication, LA-10826, 1987.
  - [6] R. Chartrand, IEEE International Conference on Image Processing, 2007.